MODEL EXPERIMENTS FOR THE DESIGN OF A SIXTY INCH WATER TUNNEL

PART II

CONTRACTION STUDIES

by

St. Anthony Falls Hydraulic Laboratory
University of Minnesota

Project Report No. 11

Submitted by

Lorenz G. Straub
Director

Prepared by

John F. Ripken
and
James S. Holdhusen

September, 1948

Prepared for the
David Taylor Model Basin
Department of the Navy
Washington, D.C.

Bureau of Ships Contract NObs-34208
Task Order 2

PREFACE TO REPORT SERIES

Contract NObs-34208 between the University of Minnesota and the Bureau of Ships, Department of the Navy, provides for making hydrodynamic studies in compliance with specific task orders issued by the David Taylor Model Basin calling for services to be rendered by the St. Anthony Falls Hydraulic Laboratory. Certain of these task orders related to model experiments for the design of a 60-in. water tunnel.

The end result of the studies related to the 60-in. water tunnel proposed eventually to be constructed at the David Taylor Model Basin was crystallized as a series of six project reports, each issued under separate cover as follows:

Part I DESCRIPTION OF APPARATUS AND TEST PROCEDURES (Project Report No. 10)

Part II CONTRACTION STUDIES (Project Report No. 11)

Part III TEST SECTION AND CAVITATION INDEX STUDIES (Project Report No. 12)

Part IV DIFFUSER STUDIES (Project Report No. 13)

Part V VANED ELBOW STUDIES (Project Report No. 14)

Part VI PUMP STUDIES (Project Report No. 15)

The investigational program was under the general direction of Dr. Lorenz G. Straub, Director of the St. Anthony Falls Hydraulic Laboratory, and the work was supervised by John F. Ripken, Associate Professor of Hydraulics.

PREFACE TO PART II

Part II of the report series was prepared in accord with Task Order 2 of Contract NObs-34208.

This report was jointly written by John F. Ripken, Associate Professor of Hydraulics, and James S. Holdhusen, Research Fellow. Mr. Holdhusen was project leader on the experimental work and was assisted by Clyde O. Johnson and Harry D. Purdy. Elaine Hulbert assisted in preparation of the manuscript.

C O N T E N T S

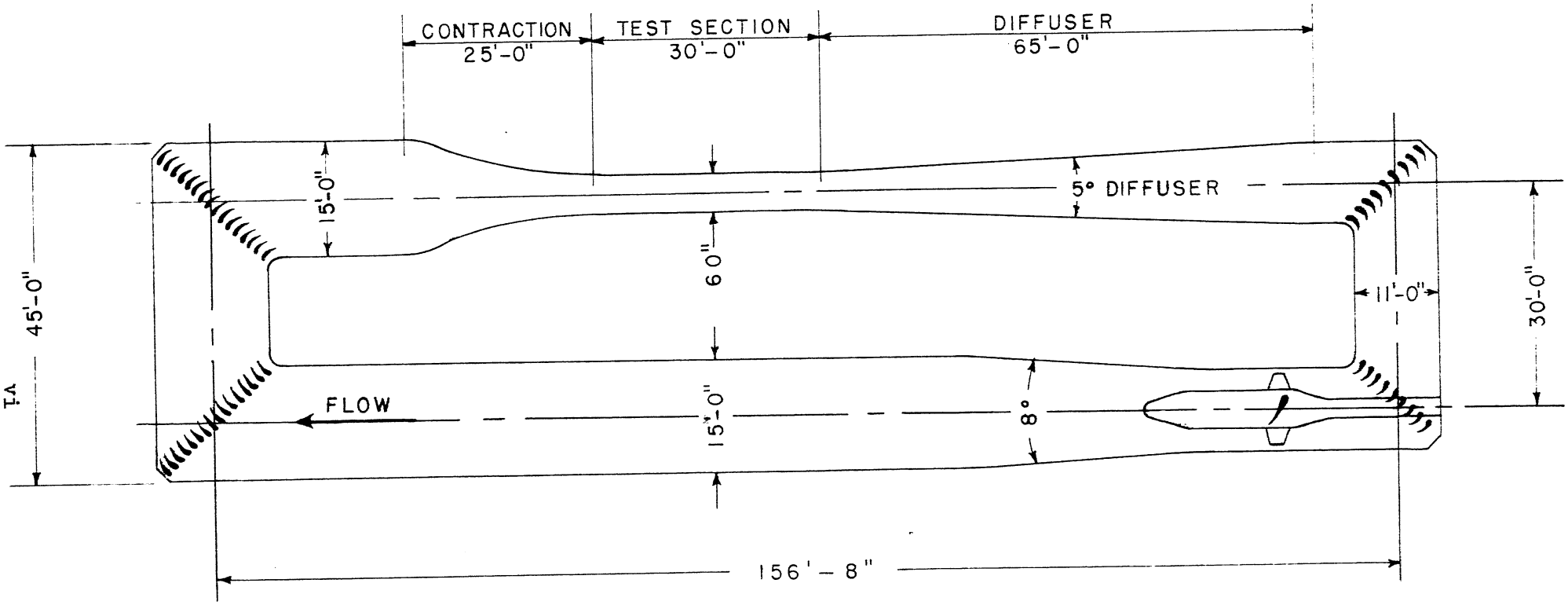

PROPOSED 60" WATER TUNNEL

CONTRACTION STUDIES

I. INTRODUCTION

A recirculating type of water tunnel is designed to produce a steady stream of fluid having uniform velocity and pressure in the test section. However, the tendency of the recirculating system is to produce variations in velocity from point to point across a section of flow due to growth of the boundary layer. Superimposed on this variation of velocity in space is a variation of velocity in time caused by turbulence in the stream. The necessity of diverting the stream through 360° and of adding energy by means of a rotary impeller introduces the possibility of superposition of steady large-scale turbulence on the stream, but correct design of elbows and pump can effectively eliminate this source of velocity variation.

It is therefore evident that some powerful corrective device must be incorporated in the tunnel circuit to eliminate these normal variations and to produce the desired quality of flow in the test section. Such a device is the contraction cone, which has been used in some form by every wind or water tunnel from the earliest model. Not only does the contracting and, later, expanding stream afford a means of attaining the desired test section flow, but it also permits reducing the power requirements of the tunnel to practicable values by reducing the velocity of flow, and therefore the head loss, in the main portion of the return circuit.

The size and amount of turbulence present in the test jet of a model testing facility has long been recognized as an important factor in the applicability of the model data to the prototype. In order to simulate prototype occurrences, in which the body moves through water containing very little turbulence, it is advisable to keep the turbulence level in the test jet as low as possible. If it does become necessary to change the intensity of turbulence in the test jet, it will be easier to add to the turbulence than to eliminate a part of it. Theory and experiment have established that a very considerable reduction in most of the turbulence components occurs when a stream passes through a contraction, the reduction being approximately proportional to the area ratio of the contraction.

II. DESIGN CONSIDERATIONS

A. Area Ratio

The corrective ability of the contraction in regard to velocity distribution may be quite easily explained and estimated by application of Bernoulli's equation along a streamline. Assuming that the contraction is preceded and followed by straight cylindrical conduits, the static pressure will be practically constant over a section of the flow at either end of the contraction. Denoting the upstream section by the subscript 1 and the downstream section by the subscript 2, the difference in pressure between the two sections will be (neglecting friction loss):

$$\frac{p_1 - p_2}{w} = \frac{\alpha_2 \bar{V}_2^2 - \alpha_1 \bar{V}_1^2}{2g} = \frac{\bar{V}_1^2}{2g} \left[\alpha_2 \left(\frac{A_1}{A_2}\right)^2 - \alpha_1\right] \qquad (1)$$

p = pressure (lb per sq ft)
w = specific weight (lb per cu ft)
$\bar{V}$ = mean velocity of flow at a cross section (ft per sec)
V = local velocity of flow on a particular streamline
g = acceleration of gravity (ft per sec^2)
A = area of flow

$$\alpha = \frac{\Sigma \Delta A V^3}{A \bar{V}^3}$$

If, now, we assume the velocity on a streamline A to be $V_{A_1} = K_A \bar{V}_1$ and the velocity on a streamline B to be $V_{B_1} = K_B \bar{V}_1$, the ratio of velocities on the same streamlines downstream of the contraction may be developed as follows:

For Streamline A:

$$\frac{p_1 - p_2}{w} = \frac{V_{A_2}^2 - V_{A_1}^2}{2g}$$

$$\text{or } V_{A_2}^2 = V_{A_1}^2 + \left(\frac{p_1 - p_2}{w}\right) 2g$$

Similarly for Streamline B:

$$V_{B_2}^2 = V_{B_1}^2 + \left(\frac{p_1 - p_2}{w}\right) 2g$$

Therefore:

$$\frac{V_{A_2}}{V_{B_2}} = \sqrt{\frac{V_{A_1}^2 + \left(\frac{p_1 - p_2}{w}\right) 2g}{V_{B_1}^2 + \left(\frac{p_1 - p_2}{w}\right) 2g}}$$

But, using $V_{A_1} = K_A \bar{V}_1$, $V_{B_1} = K_B \bar{V}_1$ and Eq. (1):

$$\frac{V_{A_2}}{V_{B_2}} = \sqrt{\frac{(K_A \bar{V}_1)^2 + \bar{V}_1^2 \left[\alpha_2 \left(\frac{A_1}{A_2}\right)^2 - \alpha_1\right]}{(K_B \bar{V}_1)^2 + \bar{V}_1^2 \left[\alpha_2 \left(\frac{A_1}{A_2}\right)^2 - \alpha_1\right]}} = \sqrt{\frac{K_A^2 + \alpha_2 \left(\frac{A_1}{A_2}\right)^2 - \alpha_1}{K_B^2 + \alpha_2 \left(\frac{A_1}{A_2}\right)^2 - \alpha_1}} \qquad (2)$$

Having established the general influence of area reduction on velocity distribution, it next becomes necessary to determine the magnitude of reduction necessary for the desired tunnel performance. The test section velocity distribution should be such that when a fixed body of model proportions (the test body) is enveloped by the moving stream, the flow mechanics between the fluid and the body are comparable to the flow mechanics of the natural prototype occurrence, in which the body is in motion and the fluid is at rest. Work in existing water and wind tunnels indicates that a velocity variation across the main body of the approaching test stream of less than one per cent is desirable. Of course, the velocity in the boundary layer must vary from zero to the velocity of the test stream, but models are made small enough so that the test section boundary layer profile does not influence the operation of the model.

In order to get some idea of the magnitude of $\frac{A_1}{A_2}$ necessary to keep the test stream velocity variation within the desired limits, it is assumed that $V_{A_1} = 1.20\,\bar{V}_1$, $V_{B_1} = 0.2\,\bar{V}_1$, $\alpha_1 = 1.07$, and $\alpha_2 = 1.00$. These values were chosen as critical since $V_{A_1} = 1.20\,\bar{V}_1$, and $\alpha_1 = 1.07$ correspond to the maximum velocity and the α value for fully developed turbulence in pipe flow; those streamlines having a velocity less than $0.2\,\bar{V}_1$ will probably be in the boundary layer at Section 2, and thus will not be expected to be within the prescribed limits of variation; and α_2 will be slightly greater than 1.0 for all flows. Consequently these values will give

the maximum value of the ratio $\frac{V_{A_2}}{V_{B_2}}$ for the main body of the jet. Values of $\frac{V_{A_2}}{V_{B_2}}$ for differing ratios of end areas obtained by substituting the assumed values in Eq. (2) are listed in Table I.

Table I	
Influence of Contraction Ratio on Uniformity of Velocity	
Area Ratio $\frac{A_1}{A_2}$	Velocity Ratio $\frac{V_{A_2}}{V_{B_2}}$
5	1.020
6	1.014
7	1.010
8	1.008
9	1.006
10	1.005

On the basis of correction of velocity variation, lowering of turbulence intensity, and economic considerations, the contraction cone was designed to have a ratio of end areas of 9:1. This contraction ratio should yield a discharge velocity variation within the prescribed limits (one per cent).

B. Wall Contour

The above conditions summarize the reasons for choosing the contraction ratio but do not give a relation that will serve as a guide in designing the boundary transition between the upstream and downstream ends of the contraction. Visual studies of plane wall orifices discharging a stream of water into the air indicate that flow naturally streamlines itself to the bellmouth type of boundary curve. The simple adoption of such a jet profile has undoubtedly served as the sole basis of many tunnel contraction cones with quite good success. However, with demands for increasing speeds and flow quality in tunnels, the simple bellmouth has generally been modified with a reverse curve that gives boundary constraint in the otherwise sharp corner.

This constraint is necessary to provide initial curvature to the approaching flow and thus eliminate the corner "dead water" eddy which forms at the entrance to the contraction when the water is allowed to determine its own approach. Elimination of this eddy is necessary at high velocities, since such eddies tend to grow progressively in size and to peel off into the passing flow. This growth and peeling is intermittent, and leads to time variations in the jet flow quality. In addition, the core of these eddies may be the cause of the small cavitation pockets at the downstream end of the contraction which have been observed in some installations.

The basis of the design of the contraction was Tsien's [1]* theoretical analysis of a wind tunnel contraction designed to avoid compressibility shock and boundary layer separation. Compressibility shock occurs only in air flows at high speeds, but its inception is under conditions analogous to those which produce cavitation in water; i.e., high local velocities exceeding the exit velocity. Tsien's reasoning is perhaps best set forth by the following summary as extracted from his paper.

> "In designing the contraction cone for a wind tunnel the usual design condition is that the velocity at the end of the cone must be fairly uniform. However, if the curvature of the wall along the flow direction is too large at certain points, local velocities at these points may exceed the uniform velocity at the end of the contraction cone. There are then regions of adverse pressure gradient and the boundary layer may separate from the wall. Furthermore, if the velocity at the end of the contraction cone is very high, say about 0.9 that of the sound, an additional factor enters--namely, the danger of compressibility shock. This danger can be avoided by keeping the velocity of flow below that of sound in the whole field of flow. In the particular case of a contraction cone, the highest velocity is reached at the wall of the cone. Therefore if the velocity at the wall is made to increase monotonically from the beginning of the cone to the end of the cone, the velocity in the cone will be always less than that of sound, provided that the velocity at the end of the contraction cone is less than the velocity of sound. The pressure will then be decreasing monotonically. Hence, the danger of boundary layer separation is also avoided."

Tsien's boundary coordinates were concerned only with the downstream portion of the contraction, and were based on a contraction ratio of 10:1. Accordingly, boundary coordinates were computed for the selected 9:1 contraction ratio, beginning at the downstream end and extending upstream until the boundary was tangent to the cylindrical conduit upstream of the contraction.

* Numbers in brackets refer to the list of references, p. 22.

It should be noted here that Tsien's analysis leads to an indeterminate solution of upstream curve coordinates except for very gradual rates of curvature, and accordingly the complete transition curve between axial tangents is somewhat longer than usual (a length of 5 test section diameters).

Computations disclosed a slight adverse pressure gradient near the upstream portion of the contraction, which, however, cannot be eliminated without making the contraction exceedingly long. The method of computing the boundary curve is contained in the original design report of the water tunnel [2], and the original computed boundary coordinates are listed in Table II, together with the dimensions of the machined aluminum casting that was actually used for the contraction of the model studies. A later recomputation of the boundary coordinates at the Taylor Model Basin disclosed some small errors: the recomputed coordinates are also listed in Table II.

III. EXPERIMENTAL STUDIES

A. Apparatus

The contraction cone in the model water tunnel consisted of a single machined aluminum casting which was attached to the upstream steel weldment approach conduit and the downstream machined aluminum test section casting by bolted flanges. The flange joints were sealed with "O" rings permitting metal-to-metal boundary continuity and were machined flush on the interior. The general relation of the contraction cone to the other tunnel elements is shown on Fig. 1.

The contraction was cast of aluminum alloy Alcoa No. 43 and with the exception of a few surface blowholes of less than 1/32-in. diameter was sound throughout.

The casting was bored using a template-following lathe and a carefully shaped metal template. The template was prepared from the original computed coordinates of Table II utilizing visual fairing and hand filing to provide a smooth curve. The template values were transferred to the casting by a special lathe set-up involving a follower device and a conventional dial indicator.

The original boring of the contraction was performed in a contract shop and resulted in a serious discrepancy in the wall contour near the downstream end. Acquisition of suitable equipment by the Hydraulic Laboratory

Table II

Coordinates of the Contraction Boundary*

Original Computed Values		Measured Values			Recomputed Values	
x	r	x	r#		x	r
0.00	8.999	0.00	9.00	Measured on template	0.00	9.000
1.33	8.932	1.50	8.95		1.34	8.955
2.67	8.699	3.00	8.75		2.68	8.781
4.00	8.366	4.00	8.47		4.02	8.382
5.33	7.699	5.00	8.11		5.36	7.754
6.67	6.986	6.00	7.62		6.70	7.021
8.00	6.199	7.00	7.08		8.04	6.299
9.33	5.699	8.00	6.50		9.38	5.658
10.67	5.166	9.00	6.02		10.71	5.111
12.00	4.733	10.00	5.58		12.05	4.644
13.33	4.333	11.00	5.21		13.39	4.286
14.67	4.000	12.00	4.88		14.73	4.018
16.00	3.746	13.00	4.56		16.07	3.736
17.33	3.586	15.00	4.04		17.41	3.521
18.67	3.400	17.00	3.68		18.75	3.360
20.00	3.300	19.00	3.41		20.09	3.239
21.33	3.200	21.00	3.25	Inside micrometer measurements	21.43	3.103
22.67	3.133	21.50	3.213		22.77	3.087
24.00	3.100	22.00	3.176		24.11	3.040
25.33	3.033	22.50	3.148		25.45	3.005
26.67	3.000	23.00	3.126		26.79	2.984
28.00	3.000	23.50	3.110		28.13	2.969
29.33	3.000	24.00	3.100		29.47	2.960
30.67	3.000	24.50	3.080		30.80	2.953
		25.00	3.070			
		25.50	3.049			
		26.00	3.033			
		26.50	3.020			
		27.00	3.013			
		27.50	3.006			
		28.00	3.003			
		29.00	3.002			
		30.00	3.002			

*Values of x are measured from the upstream end of the curve (point of tangency with cylindrical approach conduit). Values of r are radii measured from the axial center line.

#When the cone was rebored, the boundary was shifted 1/2 in. ~~upstream~~ downstream. Therefore, 1/2 in. must be added to the computed values of x before comparing the computed radii with the measured boundary radii after reboring.

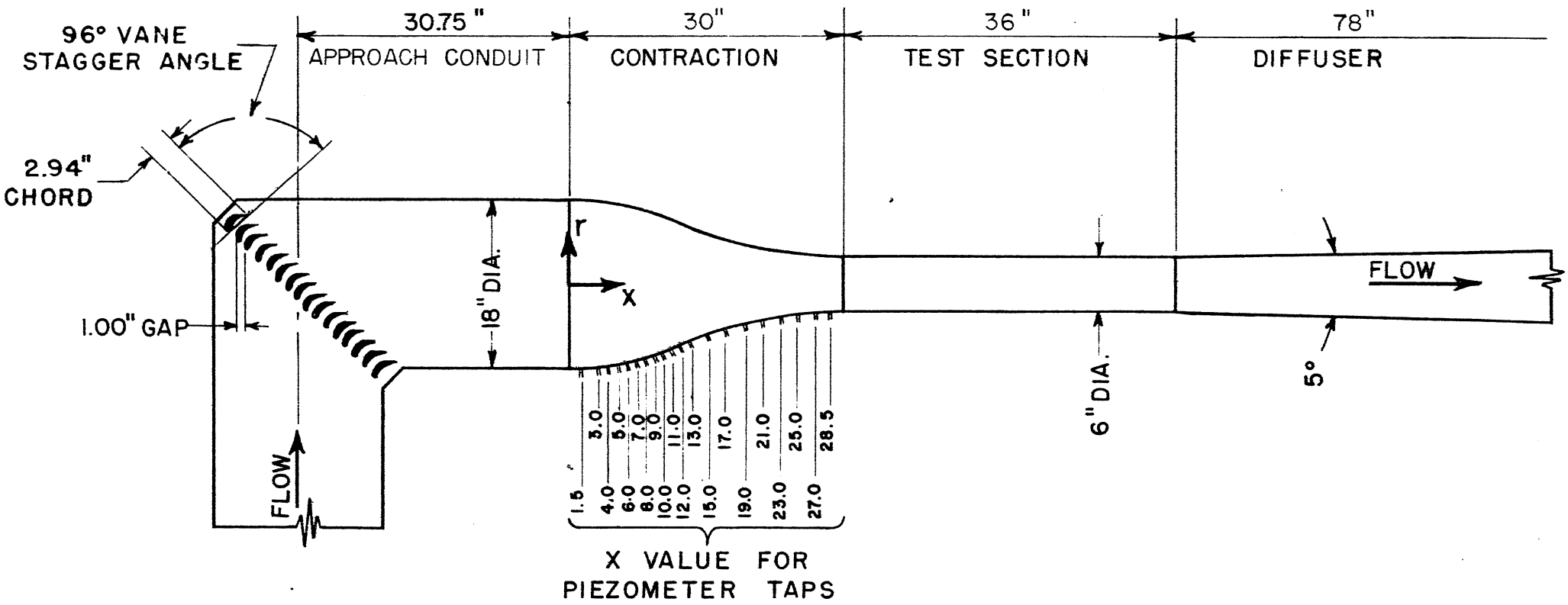

FIG. 1

SECTIONAL ELEVATION OF CONTRACTION FLOW CIRCUIT

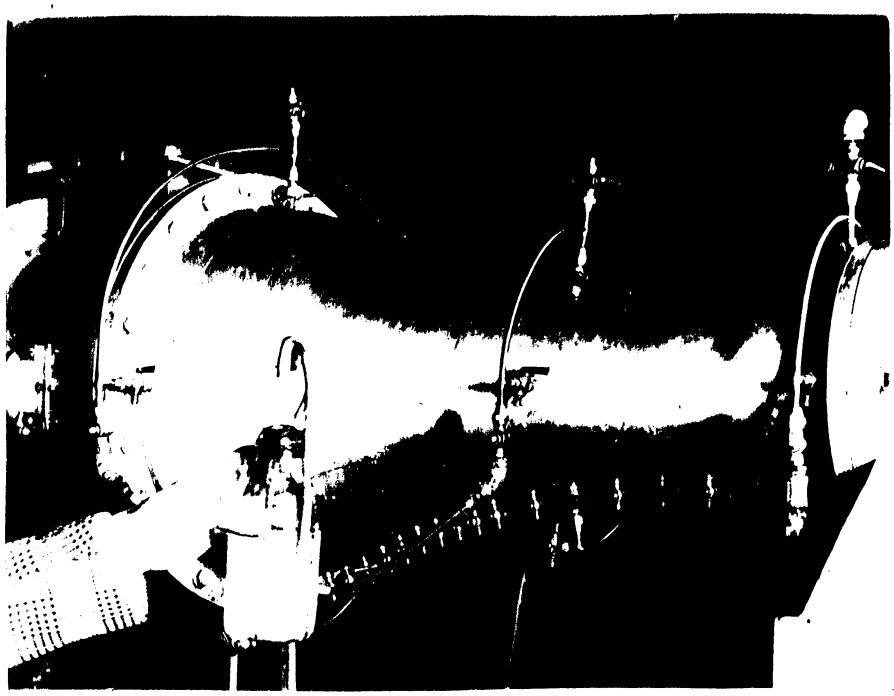

Fig. 2 Showing General Arrangement of Contraction Cone with Piezometer Taps and Flow Delineation Accessories.

permitted a reboring of the casting under controlled conditions and resulted in the measured values shown in Table II. It should be noted that this reboring resulted in an axial downstream shift of the entire contour which served to eliminate most of the discrepancy but left a slight depression of about 0.005 inches in the region of $x = 24.5$. Limited wall thickness of the existing casting prevented further machining, and time limitations prevented preparation of a new casting.

The interior finish of the casting involved smooth turning with a suitable lathe tool, followed by polishing with emery cloth, and resulted in a surface which was judged hydraulically smooth.

The casting was provided with 20 piezometer taps which were spaced along an axial line at the bottom of the cone, as shown in Figs. 1 and 2. It will be noted from Fig. 2 that three of these bottom taps were supplemented by side and top taps to yield manifold rings, which were utilized as a part of the velocity measuring instrumentation of the tunnel. Details and measurements from this feature of the contraction are given in PART I, DESCRIPTION OF APPARATUS AND TEST PROCEDURE.

The piezometer taps consisted of 1/32-in. diameter holes drilled normal to the wall and carefully deburred and chamfered at the inner end. The taps were connected by rubber tubing to 50-in. U-tube manometers.

Additional pressure data were obtained from a 3/8-in. piezometer tap located in the plane of the pitot cylinder mounting at $x = -6.0$ inches.

Velocity traverses of the flow cross section were made in two planes, one located 6 in. upstream of the contraction beginning and the other 1/2 in. downstream of the contraction end. (These traverse planes are designated as Stations 12 and 1, respectively, in other sections of this report.)

The velocity traverses were made using a 3/8-in. diameter "cantilevered" pitot cylinder in the upstream section and a 1/4-in. diameter "long" pitot cylinder in the downstream section. The details of this instrumentation are given separately in PART I, DESCRIPTION OF APPARATUS AND TEST PROCEDURE.

B. Pressure and Energy Studies

The wall pressure distributions as determined from the boundary piezometers for three different rates of flow are presented graphically in Fig. 3, with the corresponding data shown in Table III. In plotting the data, the pressure drop between the first tap (at $x = 1.50$ in.) and any other tap

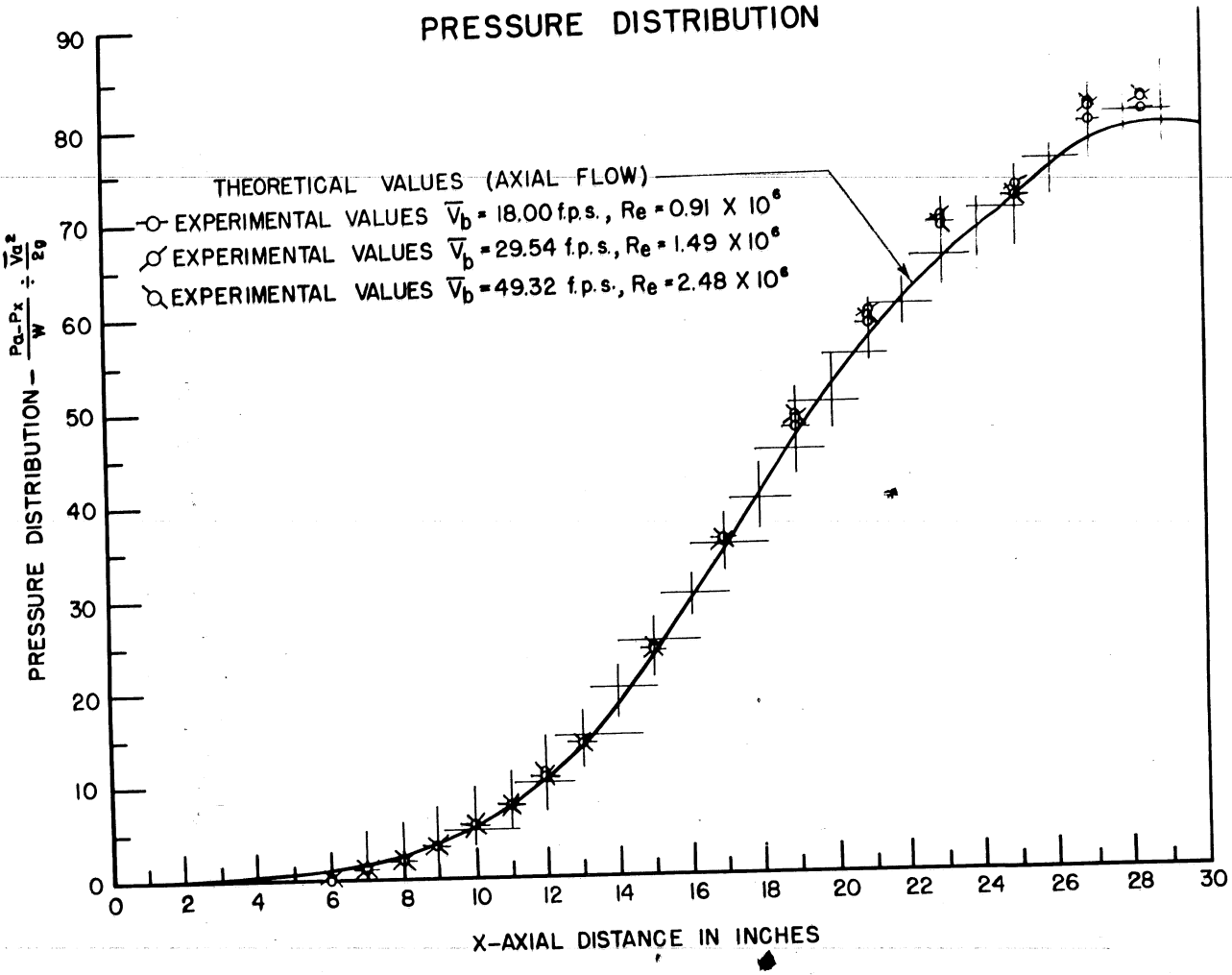

BOUNDARY CONTOUR

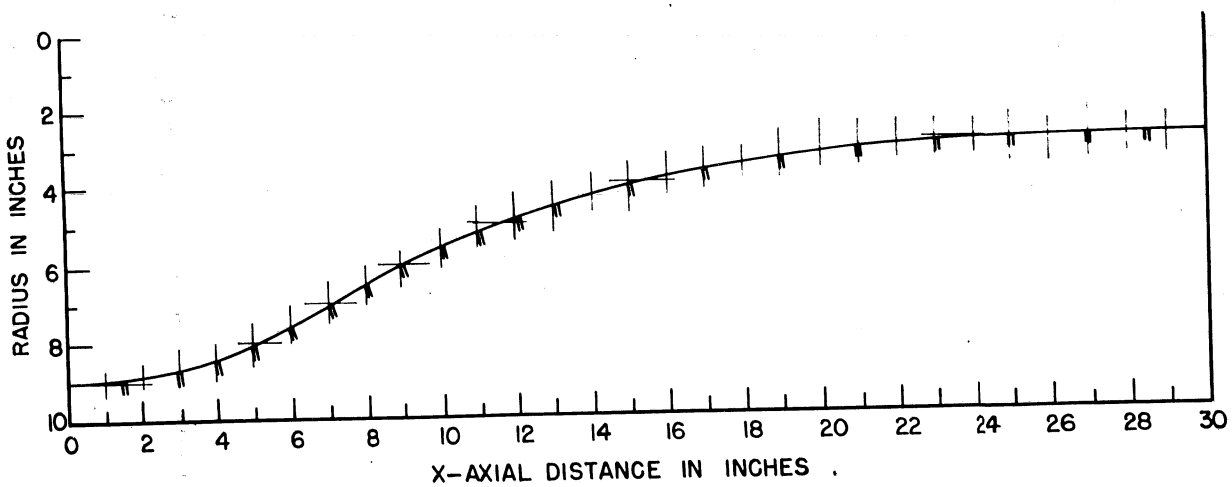

FIG. 3

PRESSURE DISTRIBUTION ALONG BOUNDARY

Table III

Boundary Wall Pressure Data

Boundary Coordinates (See Fig. 1)		Theoretical Boundary Pressure *	Experimental Boundary Pressure #		
			For $\bar{V}_z$** = 18.00 ft/sec	For $\bar{V}_z$ = 29.54 ft/sec	For $\bar{V}_z$ = 49.32 ft/sec
x (in.)	r (in.)	(K - 1)	$Re_z = 0.91 \times 10^6$	$Re_z = 1.49 \times 10^6$	$Re_z = 2.48 \times 10^6$
0.00	9.00				
1.50(a)	8.95	0.00			
3.00	8.75	0.10	0.00	0.06	0.12
4.00	8.47	0.25	0.08	0.14	0.17
5.00	8.11	0.49	0.16	0.23	0.34
6.00	7.62	0.91	0.46	0.56	0.63
7.00	7.08	1.56	1.17	1.24	1.33
8.00	6.50	2.60	2.40	2.46	2.44
9.00	6.02	3.89	3.90	3.95	3.98
10.00	5.58	5.63	5.80	5.79	5.83
11.00	5.21	7.72	7.81	7.91	7.94
12.00	4.88	10.33	10.53	10.45	10.75
13.00	4.56	13.87	14.06	14.26	14.27
15.00	4.04	23.13	24.24	24.15	24.40
17.00	3.68	34.05	35.70	35.22	35.34
19.00	3.41	46.54	47.62	48.33	48.51
21.00	3.25	56.62	58.36	59.66	58.88
23.00 ##	3.13 ##	65.97	68.57	69.00	68.40
25.00 ##	3.07 ##	71.36	71.36	72.03	71.46
27.00	3.01	77.00	79.25	80.55	80.74
28.50	3.00	78.36	80.27	81.45	81.61
30.00(b)	3.00	78.36			

* For pure axial flow with no head loss and uniform velocity distribution:

$$\text{if } K = \frac{\bar{V}_x^2}{\bar{V}_a^2} = \frac{\frac{Q^2}{\pi^2 r_x^4}}{\frac{Q^2}{\pi^2 r_a^4}} = \frac{r_a^4}{r_x^4} = \frac{(8.95)^4}{(r_x)^4}, \text{ then } \frac{p_a - p_x}{w} = \frac{(K-1)\, V_a^2}{2g}, \quad K-1 = \frac{\frac{p_a - p_x}{w}}{\frac{\bar{V}_a^2}{2g}}$$

\# All experimental pressure differences between a and x are divided by velocity head at a:

$$\frac{p_a - p_x}{w} \div \frac{\bar{V}_a^2}{2g}$$

** $\bar{V}_z$ at table heading is average velocity at contraction throat (6 in. diameter) while Re is Reynolds number based on local diameter as a length parameter.

\#\# Error in machining from x = 23.5 to 25.5.

was divided by the head of the mean velocity at Tap a (the first tap), in order to give a dimensionless plot. The solid line ("theoretical values") was computed by Bernoulli's equation, assuming purely axial flow at any section in the contraction. The wavy portion of this line between $x = 23$ and $x = 26$ results from the slight error in machining the contraction in this region.

It will be observed that no adverse pressure gradient exists downstream of $x = 1.5$. However, the pressure drop from $x = 3.0$ to $x = 9.0$ is somewhat less than would be expected from the application of Bernoulli's equation. A slight increase in pressure from the 3/8-in. tap at $x = -6.0$ to the reference tap at $x = 1.5$ was observed, amounting to approximately 9 per cent of the velocity head at $x = 1.5$. These phenomena are undoubtedly due to the concavity of the walls, which causes an increased pressure near the boundary, and are to be expected from the theory of the design. Downstream of $x = 9.0$ the measured pressure drop is consistently greater than the computed values for pure axial flow. This is explained both by the convexity of the walls and by the excess pressure drop caused by wall friction. The pressure reading at $x = 25.0$ was probably influenced by the wrinkle in the wall upstream and downstream of it, so that its deviation from the normal pattern is not surprising.

Cavitation did not occur in the contraction cone of the tunnel, even under the severest conditions of operation when cavitation was quite violent in the low pressure transition region between the test section and the diffuser.

The excess pressure drop between $x = 1.5$ and $x = 28.5$ as indicated by the difference between the measured and computed values represents closely the head loss between the upstream end of the contraction cone and the manifold at $x = 28.5$. The walls of the contraction cone are essentially parallel at the manifold so that it is not probable that any pressure drop between the two points is due to wall curvature at $x = 28.5$. The head loss between $x = 28.5$ and $x = 30$ (the end of the contraction) is computed as loss in the test section in order to simplify the computation of the test section head loss. The loss in the contraction cone, in feet, in terms of the head of the mean velocity at the exit of the contraction is $0.025 \frac{\bar{V}^2}{2g}$ at a test section velocity of 18.00 ft per sec, $0.040 \frac{\bar{V}^2}{2g}$ at a test section

velocity of 29.54 ft per sec, and $0.043 \frac{\bar{V}^2}{2g}$ at a test section velocity of 49.32 ft per sec. The reason for the increased percentage loss at higher mean velocities of flow is not apparent. Most of the energy lost in the contraction is probably due to wall friction, and this should tend to decrease with increasing Reynolds number.

In order to determine the effects of the slight negative pressure gradient previously mentioned as existing near the entrance to the contraction cone, an experimental study of the flow in the boundary layer of the contraction cone and test section was undertaken. The method of approach was very much like that employed at the Taylor Model Basin [3]. The inside surface of the contraction cone and test section was painted with a thick mixture of white lead and turpentine in the region to be investigated, and the paint was allowed to dry. About one gallon of a saturated solution of hydrogen sulfide in water was then prepared, using a commercial powder called "Aitch-Tu-Ess" to supply the gaseous H_2S. This solution was then put in a one-pint flask equipped with a two-hole stopper and rubber tube which led to the pressure tap, through which the solution was slowly fed into the tunnel while it was operating at a test section velocity of 50 ft per sec (Fig. 2). The chemical reaction between H_2S and the white lead caused the formation of black lead sulfide, which left a clearly visible record of the boundary layer flow in the vicinity and downstream of the taps. The solution was fed into four taps in the contraction cone: the tap at the top of the cone at $x = 1.5$; the tap at the bottom of the cone at $x = 4.0$; the tap at the left side of the cone (looking downstream) at $x = 17$; and the tap at the bottom of the cone at $x = 28.5$. Unfortunately, during the run the paint had flaked off the cone in the vicinity of the last tap mentioned, so that no record of the flow in this region was obtained. However, very good results were obtained by this method with the other taps used and with the tap in the test section.

Figure 4 shows the streaks left in the contraction cone after it had been taken out of the tunnel circuit. The thin black lines, which are threads taped to the wall to show the axial direction, indicate a slight counter-clockwise (looking downstream) rotation of the stream as it passes through the contraction. This rotation is not serious, however, for as indicated in Fig. 8 it does not persist to a noticeable degree in the test section. Figures 5, 6, and 7 are close-up shots of the streaks in the contraction cone. Figure 5 is probably the most noteworthy, in that it indicates

Fig. 4 Showing Nature of Boundary Wall Flow Streaks in Contraction Cone. Black Strings Represent Axial Traces.

Fig. 5 Close-Up of Flow Streak from Tap at Station x = 1.5.

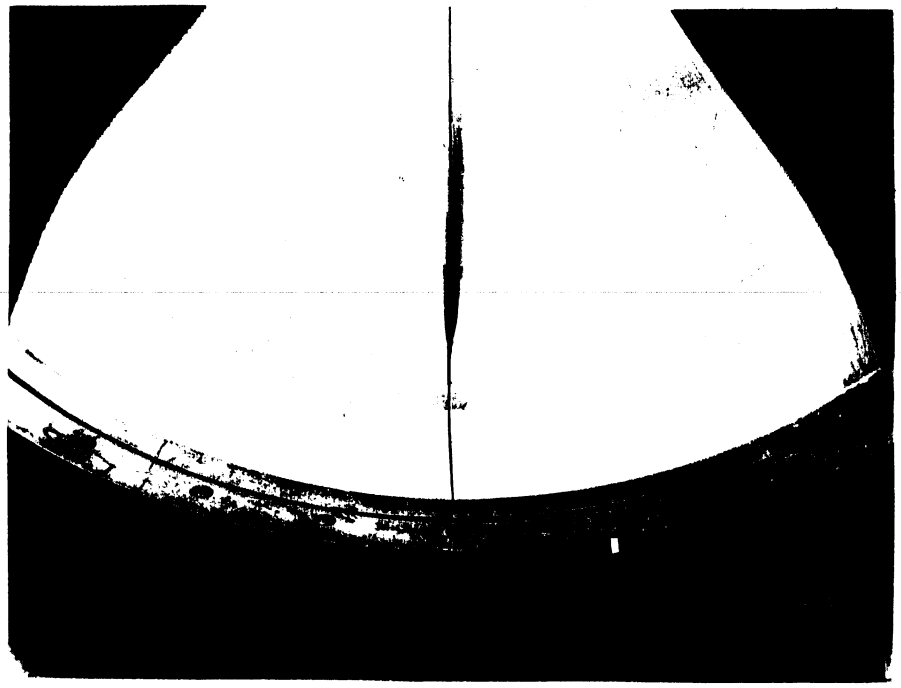

Fig. 6 Close-Up of Flow Streak from Tap at Station x = 4.0.

Fig. 7 Close-Up of Flow Streak from Tap at Station x = 17.0.

Fig. 8 Showing Nature of Boundary Wall Flow Streaks in Test Section as Viewed from Upstream End.

that some backflow separation eddying occurs near the entrance to the contraction. The indications are that the eddy is quite small and is confined to a thin part of the boundary layer, since some of the fluid is carried downstream to form the streak. The fluid near the boundary has low velocity and kinetic energy, and its pattern of flow is mainly in response to the pressure forces applied to it. Such is not the case farther away from the wall, where the kinetic energy is high enough to overcome the slight adverse pressure gradient. Evidently the solution of H_2S in water was picked up a short distance from the wall and carried downstream by the fluid which was not eddying. Further evidence that this eddy is not of serious consequence is apparent in the fact that neither cavitation nor pulsing was noticeable in the stream leaving the contraction. Figure 6 indicates that the separation eddy was confined to a small region near the entrance to the contraction, since no eddying is noticeable at this tap, which was at $x = 4.0$. Figure 7 indicates that no separation occurs in the throat of the contraction. The white line near the upper edge of the streak at its downstream end is a steel rod placed in the tap directly downstream of the point of entry of the H_2S solution in order to indicate the true axial direction. The amount of rotation of flow indicated by the streak is probably somewhat greater than that which actually existed, since the solution was heavier than water and tended to flow downward.

C. Velocity Studies

The upstream and downstream velocity distributions resulting from experimental measurements at the two traverse stations previously described are presented graphically in dimensionless form in Fig. 9 with the corresponding data given in Table IV.

These data represent measurements made at the maximum (considered most critical) velocity attainable or about 50 ft per sec. Other velocity distribution data taken at the exit station at lesser speeds are presented in PART III, TEST SECTION STUDIES but are not accompanied by the entrance distribution data as in this case because of the difficulty of accurately measuring the smaller velocities. It is noteworthy that the comparative exit velocity distributions are substantially the same regardless of speed.

Analysis of the data presented in Fig. 9 discloses the following significant indexes as applied to ultimate use of the cone in a water tunnel:

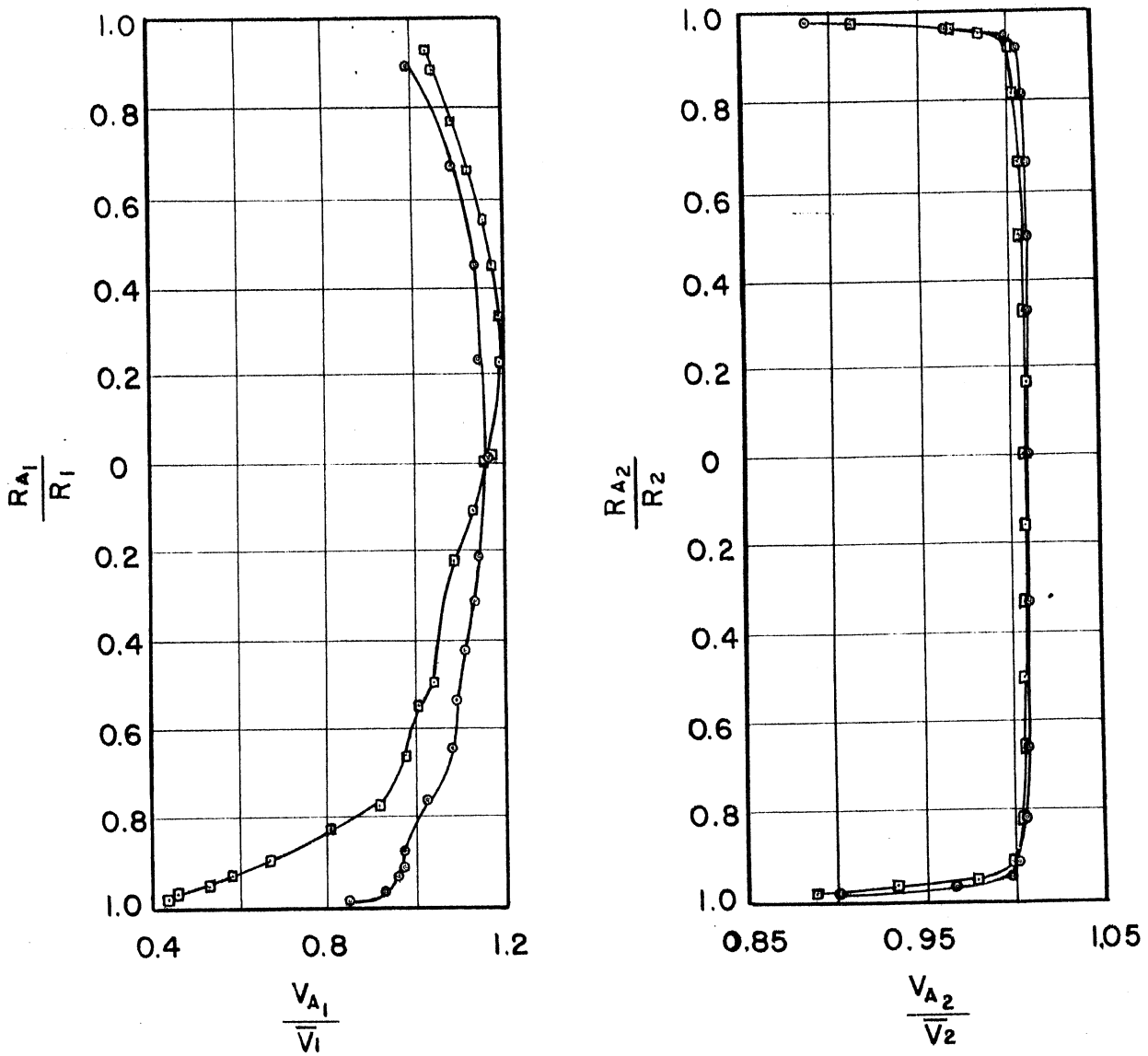

FIG. 9

CONTRACTION VELOCITY DISTRIBUTION MEASUREMENTS

TAKEN AT $\overline{V}_2$ = 49.32 f.p.s. ($R_E = 2.48 \times 10^8$)

Table IV

Velocity Distribution 6 In. Upstream of Contraction Cone

$\bar{V}_1 = 5.48$ ft per sec $Re_1 = 0.83 \times 10^6$

Horizontal Diameter (Parallel to Vanes)				Vertical Diameter (Perpendicular to Vanes)							
Distance from Side Wall (in.)	$\frac{r_{a_1}}{r_1}$	Velocity (ft per sec)	$\frac{V_{a_1}}{\bar{V}_1}$	Distance from Bottom Wall (in.)	$\frac{r_{a_1}}{r_1}$	Velocity (ft per sec)	$\frac{V_{a_1}}{\bar{V}_1}$	Distance from Bottom Wall (in.)	$\frac{r_{a_1}}{r_1}$	Velocity (ft per sec)	$\frac{V_{a_1}}{\bar{V}_1}$
0.9	0.900	5.44	0.993	0.10	0.988	2.43	0.444	13.00	0.444	6.47	1.181
2.9	.678	6.01	1.097	0.20	.978	2.52	.460	14.00	.556	6.37	1.162
4.9	.456	6.26	1.142	0.35	.962	2.92	.533	15.00	.667	6.18	1.128
6.9	.233	6.33	1.154	0.60	.933	3.18	.581	16.00	.778	6.01	1.097
8.9	.011	6.39	1.167	1.00	.888	3.68	.672	17.00	.889	5.75	1.049
10.9	.211	6.27	1.143	1.50	.833	4.46	.815	17.40	.933	5.70	1.040
11.9	.322	6.24	1.138	2.00	.778	5.06	.924				
12.9	.433	6.14	1.119	3.00	.667	5.39	.984				
13.9	.544	6.01	1.097	4.00	.556	5.53	1.008				
14.9	.656	5.96	1.088	5.50	.500	5.75	1.048				
15.9	.767	5.60	1.022	7.00	.222	5.99	1.093				
16.9	.878	5.34	.975	8.00	.111	6.22	1.135				
17.25	.916	5.34	.975	9.00	.000	6.37	1.162				
17.45	.938	5.30	.967	10.00	.111	6.47	1.181				
17.75	.972	5.11	.933	11.00	.222	6.53	1.192				
17.90	.988	4.66	.851	12.00	.333	6.53	1.192				

Velocity Distribution 1/2 In. Downstream of Contraction Cone

$\bar{V}_2 = 49.32$ ft per sec $Re_2 = 2.48 \times 10^6$

Horizontal Diameter (Parallel to Vanes)				Vertical Diameter (Perpendicular to Vanes)			
Distance from Side Wall (in.)	$\frac{r_{a_2}}{r_2}$	Velocity (ft per sec)	$\frac{V_{a_2}}{\bar{V}_2}$	Distance from Bottom Wall (in.)	$\frac{r_{a_2}}{r_2}$	Velocity (ft per sec)	$\frac{V_{a_2}}{\bar{V}_2}$
0.05	0.983	43.41	0.880	0.05	0.983	43.75	0.887
0.10	.966	47.48	0.963	0.10	.967	46.01	0.933
0.15	.950	48.88	0.991	0.15	.950	48.31	0.979
0.25	.916	49.63	1.007	0.25	.917	49.28	1.000
0.55	.817	49.84	1.010	0.55	.817	49.69	1.007
1.00	.667	49.92	1.012	1.00	.667	49.77	1.009
1.50	.500	49.92	1.012	1.50	.500	49.69	1.007
2.00	.333	49.92	1.012	2.00	.333	49.77	1.009
3.00	.000	49.92	1.012	2.50	.167	49.77	1.009
4.00	.333	49.90	1.011	3.00	.000	49.77	1.009
5.00	.667	49.77	1.009	3.50	.167	49.77	1.009
5.45	.817	49.71	1.008	4.00	.333	49.77	1.009
5.75	.917	49.36	1.001	4.50	.500	49.69	1.007
5.85	.950	49.02	0.994	5.00	.667	49.69	1.007
5.90	.967	47.69	0.968	5.45	.817	49.56	1.005
5.95	.983	44.38	0.900	5.75	.917	49.28	1.000
				5.85	.950	48.59	0.986
				5.90	.967	47.75	0.968
				5.95	.983	44.97	0.912

1. The maximum variation of velocity of the core flow at the contraction exit is of the order of 0.5 per cent, which is in accord with the design summary of Table I.

2. The thickness of the boundary layer is about 8 per cent of the exit radius, so that about 85 per cent of the area of the stream has a variation of velocity of not more than 0.5 per cent.

IV. CONCLUSIONS

On the basis of these experimental investigations, the following conclusions concerning the contraction of the 60-in. prototype tunnel are drawn:

1. The velocity variations in the test stream leaving the contraction of the prototype tunnel will be well within the prescribed maximum limit of one per cent.

2. The head loss in the prototype contraction will probably be about three per cent of the velocity head of the test stream.

3. There will be no detrimental pressure gradients or backflow in the prototype contraction except in a small region near the entrance to the cone, and the backflow there will be small enough so that it does not seriously affect the flow in the rest of the contraction.

There is no reason to believe that the slight dimensional discrepancy between the recomputed theoretical boundary and the boundary as actually tested would significantly alter the data or the above conclusions.

REFERENCES

[1] Tsien, H. S. "On the Design of the Contraction Cone for a Wind Tunnel." JOURNAL OF THE AERONAUTICAL SCIENCES, Vol. 10, February, 1943, pp. 68-70.

[2] Ripken, J. F. PRELIMINARY WATER TUNNEL DESIGN STUDIES (unpublished). David Taylor Model Basin, 1945.

[3] Hutchinson, J. F. THE DELINEATION OF SURFACE LINES OF FLOW AND WAVE PROFILES AT THE DAVID TAYLOR MODEL BASIN. Report 535, David Taylor Model Basin, May, 1944.